Nanomed. J. 7(1): 40-48, Winter 2020

RESEARCH PAPER

Use of laser-triggered gold nanoparticle-grafted dual light and temperature-responsive polymeric sensor for the recognition of thioguanine as anti-tumor agent

Kamyar Pourghazi [1*], Majid Amoli Diva [2], Mahsa Shahmirzadi [3]

[1]Department of Chemistry, Kharazmi University, Tehran, Iran
[2]School of Dentistry, Babol University of Medical Sciences, Babol, Iran
[3]Research and Development Department, Darou Pakhsh Pharmaceutical Mfg. Co, Tehran, Iran

ABSTRACT

Objective(s): Today, there is an urgent need for improved sensor materials for drug sensing and effective monitoring and interventions in this area are highly required to struggle drug abuse. The present study aimed to synthesize a thioguanine-responsive sensor based on a nanocomposite consisting of AuNP-grafted light- and temperature-responsive poly butylmethacrylate-co-acrylamide-co-methacrylic acid ([P(BMA-co-AAm-co-MAA)] with an On/Off switching property in the presence and absence of light radiation.

Materials and Methods: The incorporation of AuNPs into the structure of a polymer as the sensing moiety allows the detection of thiol-containing drug based on established gold-sulfur chemistry. The prepared nanocomposite sensor was characterized using transmission electron microscopy, scanning electron microscopy, and Fourier-transform infrared spectroscopy. In addition, the thermal sensitivity and thermal and optical switching properties of the nanocomposite were investigated. The sensor could be triggered by laser radiation at the wavelengths matched with the surface plasmon resonance (SPR) frequency of the AuNPs, providing it with an On/Off switching property.

Results: The sensor was observed to have high binding ability indicating its promising sensing applications with the wide linear responsive range of 20-250 μM and low limit of detection (0.1 μM) toward thioguanine.

Conclusion: The prepared sensor could be used to detect the analyte in biological and pharmaceutical samples, while it is also efficient in the detection of thioguanine in actual samples.

Keywords: *Au nanoparticles, Dual responsive nanocomposite, Laser, Optical sensor, Thioguanine*

How to cite this article

Pourghazi K, Amoli Diva M, Shahmirzadi M. Use of laser-triggered gold nanoparticle-grafted dual light and temperature-responsive polymeric sensor for the recognition of thioguanine as anti-tumor agent. Nanomed J. 2020; 7(1): 40-48. DOI: 10.22038/nmj.2020.07.05

INTRODUCTION

Today, the smart materials that are able to respond to external stimuli have attracted great attention. These materials have been developed and constructed to be used in various electrical and optical devices, such as sensors, switches, and drug/gene/biomaterial vehicles [1-3]. Responsive hydrogel-containing metal nanoparticles, especially those grafted to noble nanoparticles with surface plasmon resonance (SPR), have received particular attention owing to their advantageous ingredients and new properties that are available as a result of such couplings [4-6]. Gold nanoparticles (AuNPs) are particularly interesting in this regard owing to their intrinsic tunable optical properties. AuNPs are inert and biocompatible and have the SPR wavelength of approximately 530 nanometers for the NPs with the diameters of 4-40 nanometers; therefore, these NPs are viable options to be used for sensing applications [7, 8]. In fact, the binding of the target analyte to the surface of these NPs alters their SPR wavelength, which is observable by spectroscopic or colorimetric methods [9]. On the other hand, when radiation is absorbed by AuNPs at specific wavelengths, its free electrons are excited, thereby causing collective oscillation. Upon the interaction of these electrons with AuNPs crystal lattice, the electrons relax, and thermal energy is transferred to the lattice. Subsequently, the heat is dissipated to the surrounding environment

* *Corresponding Author Email: kmrpourghazi@gmail.com*
Note. This manuscript was submitted on October 15, 2019; approved on December 4, 2019

and could be used for the manipulation of the surrounding media in a controlled manner [10]. Moreover, the photo-induced heating of AuNPs could be effective in the breaking of chemical bonds, while the illuminating/heating of the NPs could trigger local phase changes or melting [11]. Since light could be easily focused to extremely small spot sizes, the possible high degree of spatial controlling could yield highly concentrated heating. As a result, optical switching could be obtained through the local generation of heat by metal NPs [12]. Recently, stimuli-responsive metallopolymers have attracted great attention for the design and development of novel materials with tunable catalytic or sensing properties. For instance, Ma et al. have presented a composite composed of poly(N-(3-amidino)-aniline) coated with AuNPs as a CO_2 sensor [13]. In another study, Wang et al. synthesized a thermo-responsive copolymer functionalized with reduced graphene oxide@Fe_3O_4@Au magnetic nanocomposites for the catalytic reduction of nitrophenol [14]. Chen et al. have also proposed the Au nanoparticle-loaded PDMAEMA brush grafted graphene oxide hybrid systems with catalytic activity [15].

Thioguanine is a member of the thiopurine group, which is widely used as an anti-tumor agent in the clinical treatment of acute childhood lymphoblastic leukemia, inflammatory bowel disease, Crohn's disease, AIDS, and other severe pathologies [16-18]. According to the literature, thioguanine inhibits the synthesis of DNA and RNA and is able to interact with the genetic material in the cells. Therefore, it has mutagenic and carcinogenic properties, while the use of this compound leads to the production of biologically harmful waste [19].In the current research, we synthesized a thioguanine-responsive sensor based on a nanocomposite consisting of AuNP-grafted light- and temperature-responsive poly butylmethacrylate-co-acrylamide-co-methacrylic acid ([P(BMA-co-AAm-co-MAA)] with an On/Off switching property in the presence and absence of light radiation. The sensing principle has been elucidated to support the sensing mechanism, volume phase transition (VPT), and thermal/optical sensitivity. The prepared sensor was applied for anti-tumor determination in biological and pharmaceutical samples, and the results confirmed the efficiency of the new strategy for the sensitive detection of thioguanine in actual samples.

MATERIALS AND METHODS

Materials

In this study, hydrogen tetrachloroaurate (III) hydrate ($HAuCl_4.3H_2O$) was purchased from Sigma (St. Louis, USA), and Merck (Darmstadt, Germany) supplied other materials, including butyl methacrylate (BMA), acrylamide (AAm), methacrylic acid (MAA), t-butyl peroctanoate (BPO), methylene bisacrylamide (MBA), sodium dihydrogen phosphate (Na_2HPO_4), potassium chloride, sodium hydroxide, trisodium citrate, hydrochloric acid, dimethylsulfoxide (DMSO), and methanol. All reagents and chemicals were of the analytical grade and used as received without further purification. In addition, deionized water was used throughout the experiments.

Instrumentation and optical setup

UV-Vis spectra were acquired using wavelength- and irradiance-calibrated Avantes Ava Spec 3648 spectrometer (Apeldoorn, Netherlands) at 200-1,100 nanometers, along with AvaLight-DH-S deuterium/halogen light source, a CUV-VAR-UV/VIS cuvette holder, and two FC-UVIR400-1ME 400 µm optical fibers. A transmission electron microscope (TEM; model: A Zeiss EM900, Oberkochen, Germany) and scanning electron microscope (SEM; model: Hitachi S-4160, Tokyo, Japan) were used for the characterization of the size and morphology of the Au NPs and nanocomposite sensor, respectively.

The adjustment of pH was performed using Metrohm 827 mV/pH meter (Herisau, Switzerland), and visible laser light was produced using a homemade 532-nanometer laser focused on top of a quartz cell. Moreover, an objective lens was mounted in front of the laser in order to focus the light beam to an approximately five-millimeter spot in diameter at the measured intensity of 630 mW cm^{-2}. Finally, the characterization of the prepared sensor was carried out using the Perkin-Elmer Spectrum and Bv5.3.0 FT-IR spectrometer within the range of 400-4,000 cm^{-1} with KBr pellets (Waltham, Massachusetts, US).

Preparation of the nanocomposite sensor

Initially, AuNPs were synthesized for the preparation of the sensor using the Turkevich approach through the controlled reduction of aqueous gold salt using trisodium citrate in accordance with our previously reported methodology [20]. In brief, 40 ml of deionized

water was added to chloroauric acid (5 ml, 5 mM) in a conical flask, and the combination was heated to boil with constant magnetic stirring for 15 minutes. Afterwards, trisodium citrate (5 ml, 50 mM) was added to the solution, and the color of the solution changed from almost colorless to deep red immediately. The mixture was heated again for 10 minutes and rapidly cooled in an ice bath. The TEM image of the prepared AuNPs (Fig 1) revealed spherical particles with the mean diameter of 9±2 nanometers, which was stable for a minimum of three months.

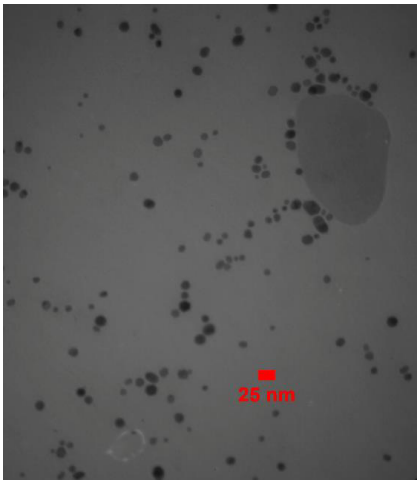

Fig 1. TEM image of prepared AuNPs (mean diameter: 9±2 nm)

In the next stage, the BMA, AAm, and MAA monomers (0.01, 0.05, and 0.05 M, respectively) and AuNPs (5 ml, 0.2 mM) were added to DMSO:methanol solution (50 ml, 1:1 v/v) in a 100-ml, three-necked, round-bottom flask equipped with an N_2 gas inlet, a condenser, and a thermometer. Following that, 0.20 gram of MBA and 0.1 milliliter of BPO were added to the mixture as the cross-linkers during the constant magnetic stirring. The solution was degassed by the N_2 gas for a minimum of 20 minutes, and polymerization initiated at the temperature of 80ºC for 10 hours. Following that, the mixture was cooled to the room temperature, and the supernatant was decanted. The nanocomposite was suspended in 10milliliters of methanol, stirred with a glass stirrer, centrifuged at 2,150 g for five minutes, and re-suspended in methanol; this procedure was repeated five times. Afterwards, the nanocomposite was immersed in 50 ml of methanol for 24 hours, and the solvent was changed every six hours in order to remove the non-reactive chemicals and monomers. Finally, the solid product was obtained in the form of a pale pink powder after drying in an oven at the temperature of 40ºC.

Stability of the sensor in different conditions

For biological applications, the sensor should be stable under different conditions. The stability of the prepared nanocomposite was evaluated based on the aggregation parameter, which was determined by the variation of the integrated absorbance within the range of 600-700 nanometers [21, 22]. The parameter was defined using the following equation:

$Aggregation\ Parameter=(A-A_0)/A_0$

where A_0 and A represent the integrated absorbance of the nanocomposite before and after each condition (i.e., ionic strength and pH).

The effect of ionic strength was evaluated by adding various concentrations of sodium chloride (0-200 mM; pH=7), and the effect of pH was investigated using various buffered solutions within the range of 3-10.

Swelling and VPT measurement of the sensor

The swelling of the prepared nanocomposite was investigated at various temperatures using the gravimetric method as reported previously [23]. In brief, a weighed amount of the nanocomposite was placed in 50 ml of deionized water at the desired temperature for 30 minutes. Following that, the sample was removed and blotted with filter paper in order to remove the excess surface water and weighed again. The swelling ratio was calculated using the following equation:

$Swelling\ Ratio=(W_s - W_n)/W_n$

where W_s is the weight of the swollen sensor, and W_n denotes the weight of the nanocomposite before swelling.The mean values obtained by the measurements were reported at each temperature. In addition, the thermal sensitivity or VPT temperature of the nanocomposite was evaluated through transmittance measurement at various temperatures (10-60°C) of the aqueous solution. At this stage, 0.2 gram of the nanocomposite in three ml of deionized water was transferred to a 3.5-ml quartz cell and placed in a water bath, which was adjusted to the desired temperature, and its transmittance was measured immediately.

Thermal and optical switching capability

The thermal switching properties of the prepared sensor were measured using 0.2 gram

of the nanocomposite, which was suspended in three ml of deionized water and preheated to the temperature of 40ºC as it is close to its VPT temperature. Afterwards, the sample was heated to the temperature of 60ºC for 60 seconds and left in an ambient temperature for passive cooling. Two cycles were performed, and the second cycle was initiated four minutes after the start of this stage. The duration of the entire experiment was eight minutes, and the reported value was an average of three replicates at each temperature.

The optical switching property of the prepared nanocomposite was evaluated using a similar procedure to the measurement of thermal switching, with the exception that the required heat for phase transition was supplied by light radiation. To do so, the samples were pre-heated to the temperature of 40ºC and illuminated using a 532-nanometer diode laser for 60 seconds, followed by passive cooling to the room temperature so as to reach the minimum transmittance. Two cycles were performed, and the second cycle was initiated four minutes after the start of this stage. The duration of the entire experiment was eight minutes, and the reported value was an average of three replicates at each temperature.

Detection of thioguanine

The stock solution of the analyte (1.0 mM) was prepared by dissolving proper amounts of thioguanine in methanol, and the solution was prepared by diluting the stock solution with deionized water. In order to detect thioguanine, 0.2 gram of the nanocomposite was added to three ml of various concentrations of the analyte at the path-length cell of one centimeter at the room temperature. The absorption spectra were recorded within the range of 400-800 nanometers before and after laser beam radiation at 532 nanometers and various times.

Preparation of real samples

At this stage, urine samples were obtained from healthy volunteers aged 25-40 years and stored at the temperature of 4ºC. Following that, five ml of the samples were mixed with 1.0 ml of methanol and centrifuged at 3,000 rpm for 15 minutes. In addition, five ml of the clear supernatant was diluted to 50 ml. Recovery tests were performed by the addition of appropriate concentrations of the thioguanine solution to the samples, and the proposed model was applied.

Plasma samples of healthy volunteers aged 25-35 years were also obtained from the Iranian Blood Transfusion Organization and stored at the temperature of -16ºC. During the analysis, the samples were transferred to an oven and preserved at the temperature of 37ºC for two hours. Afterwards, five ml of each sample and 1.0 ml of methanol were centrifuged at 3,000 rpm for 15 minutes, and five ml of the clear supernatant was spiked with appropriate concentrations of the thioguanine solution before dilution to 50 ml.

In total, 20 thioguanine tablets labeled with 40 mg of the analyte per tablet were weighed, their mean weight was calculated, and the samples were finely powdered. A portion of the powder that was equivalent to one tablet was accurately weighed and dissolved in 100 ml of methanol. Afterwards, the solution was filtered using a filter paper (Whatman no. 1), and 1.0 ml of the solution was diluted to 50 ml using deionized water. Furthermore, the standard addition method was used for the detection of the anti-tumor drug in the actual samples.

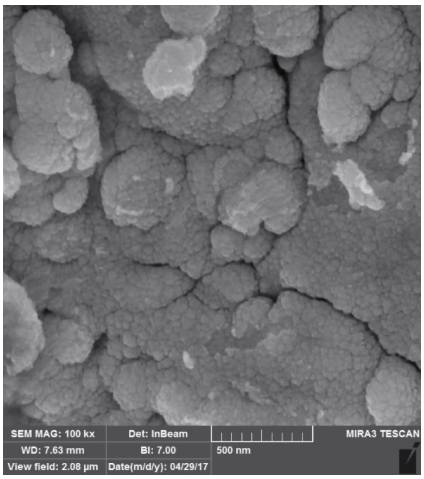

Fig 2. SEM image of prepared nanocomposite (mean diameter: 85±8 nm)

RESULTS AND DISCUSSION

The present study aimed to synthesize an upper critical solution temperature (UCST)-based dual light and temperature-responsive polymeric sensor using AuNPs as the core, so that it could act as a tunable optical switch, in which the "On state" denotes illumination by specific SPR wavelengths, while "Off state" shows that the light has been turned off. This SPR wavelength is larger than the lowest inter-band transition of Au

at 470 nanometers [24]. As such, the absorbed energy converts into heat and is dissipated to the surrounding polymeric environment, thereby resulting in increased body temperature and VPT. This is followed by chain opening (On state of the sensor), diffusing of the analyte to the polymeric shell, and its binding to the AuNP core. Moreover, the electrostatic interactions between the carboxylic acid groups of the MAA units and amine group of thioguanine acted as the driving force for the binding of the analyte to the sensor. In this state, turning off the light leads to temperature decline and de-swelling of the polymeric chain, finally causing drug departure. The efficiency of the sensor could be determined by the monitoring of the UV-Vis absorbance changes in thioguanine.

Characterization of the nanocomposite

SEM images indicated the size and morphology of the prepared nanocomposite. As can be seen in Fig 2, the prepared nanocomposite had relatively uniform size distribution with the mean diameter of 85±8 nanometers, and most of the particles were quasi-spherical.

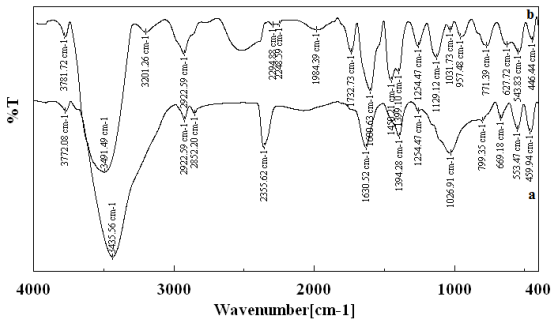

Fig 3. FTIR spectra of a) Polymer alone and b) nanocomposite

Fig 3 shows the FTIR spectra of the plain responsive polymer and prepared nanocomposite. As can be seen, the stretching vibration of C=O belonged to the carboxylic acid in the MAA monomer, which could be observed at approximately 1630-1730 cm^{-1}. In addition, the stretching vibration of the C-N bond in the AAm and MBA units was observed at 1026 cm^{-1}, and the C-N absorption band appeared at 957 cm^{-1}, which shifted to the lower wave numbers, indicating the coordinative chemical bonding of C-N to the AuNPs. On the other hand, the weak absorption bands at approximately 2922 and 2852 cm^{-1} were attributed to the stretching vibration of the methylene groups, while the absorption band at 3430-3450 cm^{-1} was attributed to the OH and/or NH_2 functional groups of the polymer or hydroxyl group of the absorbed water. According to the obtained results, all the monomers were incorporated into the polymeric structure, and the AuNPs were attached to the polymer.

Stability of the sensor under different conditions

The effects of ionic strength and pH on the stability of the prepared sensor were investigated using various concentrations of sodium chloride (0-200 mM; pH=7) and different buffered solutions (range 3-10) in the prepared nanocomposite. Fig 4 shows the variations of the aggregation parameter at various pH levels. As can be seen, the nanocomposite was stable at basic, neutral, and slightly acidic pH levels. However, its aggregation started at lower pH than six as evidenced by the increment in the aggregation parameter.

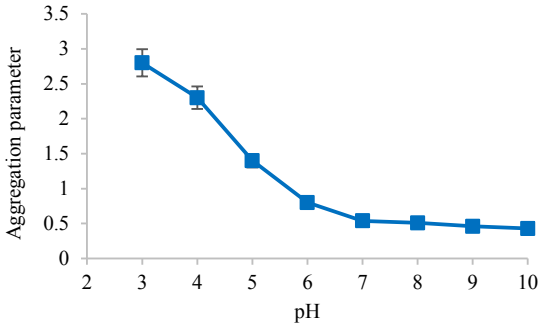

Fig 4. Stability of nanocomposite at various pH values

In the present study, the poly MAA in the structure of the polymeric segment was observed to be a weak polycarboxylic acid with pK_a of approximately six [25]. At the levels below this pK_a value, almost all the carboxylic acid groups in the structure were in the form of COOH, while the polymer was in its neutral form. As a result, the electrostatic repulsion between the monomers reduced.

The aggregation was reversible, and the addition of the basic solution resulted in the complete recovery of the initial spectrum.

According to the results of the ionic strength and stability measurements, the prepared nanocomposite was stable in the sodium chloride solutions up to 120 mM with no obvious changes in the absorbance spectrum. Moreover, the aggregation induced by higher sodium chloride concentrations was attributed to the absorbance at 532 nanometers, and its increment was denoted at higher wavelengths.

Swelling measurements

Fig 5 depicts the temperature dependence of nanocomposite swelling in deionized water. As shown, positive swelling was observed with increased temperature.

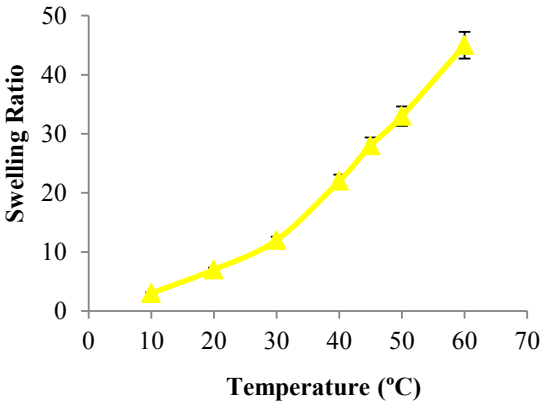

Fig 5. Swelling behavior of nanocomposite in deionized water at various temperatures

At low temperatures, the hydrogen bonds that were established between the functional groups of the monomeric units led to inter-polymer interactions/complexation, thereby resulting in polymer collapse and insolubility of the nanocomposite, which decreased the swelling ratio. High temperatures dissociate these bonds, allowing the solvent to penetrate into the structure and increase the swelling ratio. At low temperatures, the building blocks of the hydrogel are able to form continuous ladder-like interactions, which are composed of numerous AAm-MAA units [26] and could lead to the shrinkage of the polymer. With increased temperature, some complex units may start to dissociate through the dissociation of hydrogen bonds, thereby promoting the cooperative dissociation of the adjacent complexes due to potent hydration forces.

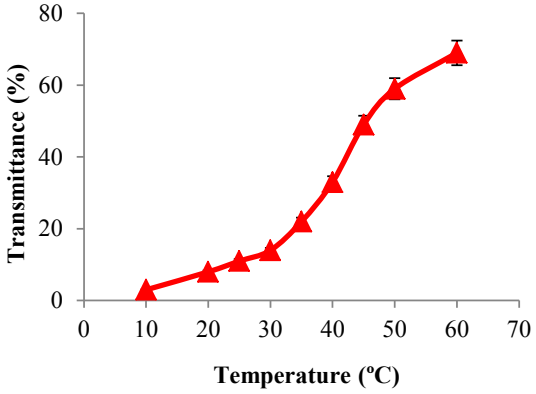

Fig 6. VPT temperature of nanocomposite in deionized water

Fig 6 shows the temperature dependence of transmittance or VPT temperature measurement of the prepared nanocomposite. As stated earlier, higher pH than pK_a caused the carboxyl groups of the polymeric structure to ionize, and the repulsive forces between the same charged groups led to the swelling and dispersion of the nanocomposite in the solution. With increased temperature, the nanocomposite underwent a VPT from the shrunk sate to the swollen state. In fact, the BMA units in the polymeric segment of the sensor contained hydrophobic molecules, and the driving force for this temperature-sensitive VPT was attributed to the balance established in the hydrophobic/hydrophilic interactions between the network chains and water molecules.

Thermal and optical switching

The thermal and optical switching of the prepared nanocomposite was investigated in two cycles (Fig 7). In both experiments, the transmittance increased after heating/radiation and reached the maximum within approximately 60 seconds. In addition, the behavior of the nanocomposite in the optical switching experiments was similar to thermal switching. Both experiments were indicative of reversible switching with different phase-back times; thermal switching showed longer phase-time for total collapse after turning off the heat in terms of optical switching. On the other hand, transmittance drop was observed to be more rapid after turning off the light, which could be due to the efficient heat conduction of the NPs in terms of the polymeric structure. In optical switching, the required temperature for phase transition was supplied by the local heat generated by the AuNPs through irradiation at the SPR wavelength.

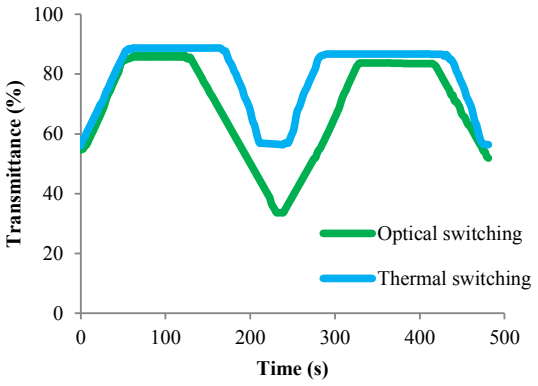

Fig 7. Thermal and optical switching properties of nanocomposite sensor

Table 1. Comparison of proposed method for detection of thioguanine with some sensor-based methods previously reported

Sensor type	Method	Linear range (μM)	LOD (μM)	Ref.
Pt/MWCNTs	Square Wave Voltammetry	0.1-500	0.05	[27]
Harmine-modified silver nanoparticles	Fluorescence resonance energy transfer	0.015-75	0.009	[28]
dsDNA/ 2-aminoethanethiol film-modified gold electrode (AET/Au SAMs)	Surface electrochemical method with $[Fe(CN)_6]$ probe	1.1-110	0.2	[29]
dsDNA/ 2-aminoethanethiol film-modified gold electrode (AET/Au SAMs)	Surface electrochemical method with $Co(bpy)_3$ probe	0.4-220	0.12	[29]
NiO nanoparticle-modified carbon-paste electrode	Square-wave voltammetry	0.09–300.0	0.06	[30]
AuNP-grafted polymer	Spectrophotometry	20-250	0.1	This work

Table 2. Results for detection of thioguanine in real samples (n=5)

Sample	Added (μM)	Found (μM)±%RSD	Recovery (%)
Plasma	0	<LOD	-
	20.0	18.34±2.4	91.7
	100.0	95.12±4.1	95.1
	200.0	192.61±3.9	96.3
Urine	0	<LOD	-
	20.0	18.68±3.2	93.4
	100.0	94.53±3.7	94.5
	200.0	192.8±4.5	96.4
Tablet	0	7.81±1.1	-
	20.0	27.31±2.3	98.2
	100.0	111.15±4.0	103.1
	200.0	212.59±4.3	102.3

Moreover, the light energy absorbed by the NPs was dissipated as heat to the surrounding environment and absorbed by the temperature-responsive polymer around the NPs. The other findings in this regard indicated the suitability of the prepared nanocomposite as an efficient optical switch in various industries.

Analytical parameters

The prepared sensor was applied for the detection of thioguanine in a buffered solution (pH=7). The sensor had a linear response within the range of 20-250 μM, with the correlation-coefficient estimated at 0.992 and the limit of detection (LOD) calculated to be 0.1 μM based

on $3S_b$ (S_b as the standard deviation of the seven-time blank analysis). It is notable that the relative standard deviation (RSD) was calculated as the precision factor for the five-time analysis of thioguanine (50 mM), and the acceptable precision of 4.3% was achieved. These findings are consistent with the previous studies regarding the detection of thioguanine (Table 1).

Interference studies

The effects of the presence of various materials that may potentially interfere in the detection of thioguanine were investigated using 50 µM of the analyte solution. Moreover, the compounds or ions that may be commonly found along with thioguanine in pharmaceutical or biological fluids at different concentrations were added to the solution in the presence of the nanocomposite. The maximum concentration of the co-existing materials that could lead to the RSD of less than 5.0% for the recovery of thioguanine was considered as the maximum tolerance limit. Furthermore, the obtained results revealed that the recovery of the analyte was not affected by the presence of the 10-fold concentration of sucrose, glucose, lactose, fructose, benzoic acid, PEG, L-lysine, L-asparagine, glycine, ethanol, and methanol and the 100-fold concentration of Fe^{3+}, Mg^{2+}, NH_4^+, and SO_4^{2-}, which suggested the proper selectivity of the method.

Analysis of the real Samples

In order to evaluate the applicability of the prepared sensor in real samples, it was used to detect thioguanine in biological fluids (human urine and plasma samples) and pharmaceutical samples (commercial tablets). The nanocomposite (0.2 g) was transferred to three ml of each biological/pharmaceutical sample, spiking at various concentrations of the analyte. In addition, laser radiation was applied for two minutes, and the absorbance spectrum of the supernatant was immediately recorded before turning off the laser. The measurements were performed in five replicates, and the obtained results are presented in Table 2. According to the results presented in this table, the recovery range was determined to be 91.7-103.1%, indicating no significant interference in the analysis of the actual samples. Furthermore, the RSDs were estimated to be less than 4.3%, which confirmed the acceptable reproducibility of the proposed method. In addition, the experimental results indicated that the prepared sensor could be applied for the detection of thioguanine in actual samples.

CONCLUSION

The current research involved the successful synthesis of a new polymeric sensor with dual light and temperature responsiveness, the structure of which consisted of SPR-based AuNPs and a switching property. The synthesized nanocomposite exhibited a specific response to thioguanine as the model drug in response to radiation at the SPR of the NPs. The prepared sensor was characterized using TEM, SEM, and FTIR, and its thermal sensitivity and thermal and optical switching properties were investigated as well. Finally, assays for the measurement of the anti-tumor drug in the human plasma and urine samples and commercial tablets were developed with the prepared nanocomposite employed as the sensing probe. According to the obtained results, the recoveries were within the range of 91.7-103.1% with the precision (i.e., RSD%) of less than 4.3%. Furthermore, the findings denoted that the prepared sensor potentially has numerous applications in pharmaceutical and medical industries.

ACKNOWLEDGMENTS

Hereby, we would like to thank Dr. Mitra Amoli Diva for their cooperation and supplying some equipments.

REFERENCES

1. Jean R-D, Larsson M, Cheng W-D, Hsu Y-Y, Bow J-S, Liu D-M. Design and optimization of a nanoprobe comprising amphiphilic chitosan colloids and Au-nanorods: Sensitive detection of human serum albumin in simulated urine. Appl Surface Sci. 2016; 390: 675-680.
2. Ding Y, Shen SZ, Sun H, Sun K, Liu F, Qi Y, Yan J. Design and construction of polymerized-chitosan coated Fe3O4 magnetic nanoparticles and its application for hydrophobic drug delivery. Mater Sci Engin C. 2015; 48: 487-498.
3. Karfa P, Roy E, Patra S, Kumar D, Madhuri R, Sharma PK. A fluorescent molecularly-imprinted polymer gate with temperature and pH as inputs for detection of alpha-fetoprotein. Biosensor Bioelectron. 2016; 78: 454-463.
4. Amoli-Diva M, Sadighi-Bonabi R, Pourghazi K. Laser-assisted triggered-drug release from silver nanoparticles-grafted dual-responsive polymer. Mater. Sci. Engin. C. 2017;76:536-542.
5. Wang Y-C, Lu L, Gunasekaran S. Biopolymer/gold nanoparticles composite plasmonic thermal history indicator to monitor quality and safety of perishable bioproducts. Biosensor Bioelectron. 2017; 92: 109-116.
6. Shu T, Lin X, Zhou Z, Zhao D, Xue F, Zeng F, Wang J, Wang

C, Su L, Zhang X. Understanding stimuli-responsive oligomer shell of silver nanoclusters with aggregation-induced emission via chemical etching and their use as sensors. Sensor Actuat B. 2019; 286: 198-205.
7. Sperling RA, Rivera Gil P, Zhang F, Zanella M, Parak WJ. Biological applications of gold nanoparticles. Chem Soc Rev. 2008; 37(9): 1896-1908.
8. La JA, Lim S, Park HJ, Heo M-J, Sang B-I, Oh M-K, Cho EC. Plasmonic-based colorimetric and spectroscopic discrimination of acetic and butyric acids produced by different types of Escherichia coli through the different assembly structures formation of gold nanoparticles. Anal Chim Acta. 2016; 933: 196-206.
9. Zheng L, Wei J, Lv X, Bi Y, Wu P, Zhang Z, Wang P, Liu R, Jiang J, Cong H, Liang J, Chen W, Cao H, Liu W, Gao GF, Du Y, Jiang X, Li X. Detection and differentiation of influenza viruses with glycan-functionalized gold nanoparticles. Biosensor Bioelectron. 2017; 91: 46-52.
10. Langhammer C, Kasemo B, Zoric I, Larsson E. Sensor using localized surface plasmon resonance (lspr). Google Patents; 2012.
11. Kono K, Takeda K, Li X, Yuba E, Harada A, Ozaki T, Mori S. Dually functionalized dendrimers by temperature-sensitive surface modification and gold nanoparticle loading for biomedical application. RSC Adv. 2014; 4(53): 27811-27819.
12. Huang X, El-Sayed MA. Gold nanoparticles: Optical properties and implementations in cancer diagnosis and photothermal therapy. J Adv Res. 2010; 1(1): 13-28.
13. Ma Y, Promthaveepong K, Li N. CO2-Responsive Polymer-Functionalized Au Nanoparticles for CO2 Sensor. Anal Chem. 2016; 88(16): 8289-8293.
14. Wang D, Duan H, Lu J, Lu C. Fabrication of thermo-responsive polymer functionalized reduced graphene oxide@Fe3O4@Au magnetic nanocomposites for enhanced catalytic applications. J Mater Chem A. 2017; 5(10): 5088-5097.
15. Chen J, Xiao P, Gu J, Huang Y, Zhang J, Wang W, Chen T. Au nanoparticle-loaded PDMAEMA brush grafted graphene oxide hybrid systems for thermally smart catalysis. RSC Adv. 2014; 4(84): 44480-44485.
[16. Hasanzade Z, Raissi H. Solvent/co-solvent effects on the electronic properties and adsorption mechanism of anticancer drug Thioguanine on Graphene oxide surface as a nanocarrier: Density Functional Theory Investigation and A Molecular Dynamics. Appl Surface Sci. 2017.
17. Mirmomtaz E, Ensafi AA. Voltammetric determination of trace quantities of 6-thioguanine based on the interaction with DNA at a mercury electrode. Electrochim Acta. 2009; 54(18): 4353-4358.
18. Beitollahi H, Ivari SG, Torkzadeh-Mahani M. Voltammetric determination of 6-thioguanine and folic acid using a carbon paste electrode modified with ZnO-CuO nanoplates and modifier. Mater Sci Engin C. 2016; 69: 128-133.
19. Ensafi AA, Hajian R. Simultaneous determination of captopril and thioguanine in pharmaceutical compounds and blood using cathodic adsorptive stripping voltammetry. J Brazil Chem Soc. 2008; 19: 405-412.
20. Beiraghi A, Pourghazi K, Amoli-Diva M. Au nanoparticle grafted thiol modified magnetic nanoparticle solid phase extraction coupled with high performance liquid chromatography for determination of steroid hormones in human plasma and urine. Anal Method. 2014; 6(5): 1418-1426.
21. Qiao J, Ding H, Liu Q, Zhang R, Qi L. Preparation of Polymer@AuNPs with Droplets Approach for Sensing Serum Copper Ions. Anal Chem. 2017; 89(3): 2080-2085.
22. Lévy R, Thanh NTK, Doty RC, Hussain I, Nichols RJ, Schiffrin DJ, Brust M, Fernig DG. Rational and Combinatorial Design of Peptide Capping Ligands for Gold Nanoparticles. J Am Chem Soc. 2004; 126(32): 10076-10084.
23. Amoli-Diva M, Pourghazi K, Mashhadizadeh MH. Magnetic pH-responsive poly(methacrylic acid-co-acrylic acid)-co-polyvinylpyrrolidone magnetic nano-carrier for controlled delivery of fluvastatin. Mater Sci Engin C. 2015; 47: 281-289.
24. Etchegoin PG, Le Ru EC, Meyer M. An analytic model for the optical properties of gold. J Chem Phys. 2006; 125(16): 164705.
25. Guo W, Hu N. Interaction of myoglobin with poly(methacrylic acid) at different pH in their layer-by-layer assembly films: an electrochemical study. Biophys Chem. 2007; 129(2-3): 163-171.
26. Katono H, Maruyama A, Sanui K, Ogata N, Okano T, Sakurai Y. Thermo-responsive swelling and drug release switching of interpenetrating polymer networks composed of poly(acrylamide-co-butyl methacrylate) and poly (acrylic acid). J Control Rel. 1991;16(1): 215-227.
27. Karimi-Maleh H, Shojaei AF, Tabatabaeian K, Karimi F, Shakeri S, Moradi R. Simultaneous determination of 6-mercaptopruine, 6-thioguanine and dasatinib as three important anticancer drugs using nanostructure voltammetric sensor employing Pt/MWCNTs and 1-butyl-3-methylimidazolium hexafluoro phosphate. Biosens. Bioelectron. 2016; 86: 879-884.
28. Amjadi M, Farzampour L. Selective turn-on fluorescence assay of 6–thioguanine by using harmine-modified silver nanoparticles. Luminescence. 2014; 29(6): 689-694.
29. Wang W, Wang S-F, Xie F. An electrochemical sensor of non-electroactive drug 6-thioguanine based on the dsDNA/AET/Au. Sensor Actuat B. 2006; 120(1): 238-244.
30. Karimi-Maleh H, Salimi-Amiri M, Karimi F, Khalilzadeh MA, Baghayeri M. A Voltammetric Sensor Based on NiO Nanoparticle-Modified Carbon-Paste Electrode for Determination of Cysteamine in the Presence of High Concentration of Tryptophan. J Chemistry. 2013; 2013: 7.